

J0815+4729: A CHEMICALLY PRIMITIVE DWARF STAR IN THE GALACTIC HALO OBSERVED WITH
GRAN TELESCOPIO CANARIAS. *

DAVID S. AGUADO,^{1,2} JONAY I. GONZÁLEZ HERNÁNDEZ,^{1,2} CARLOS ALLENDE PRIETO,^{1,2} AND RAFAEL REBOLO^{1,2,3}

¹*Instituto de Astrofísica de Canarias, Vía Láctea, 38205 La Laguna, Tenerife, Spain*

²*Universidad de La Laguna, Departamento de Astrofísica, 38206 La Laguna, Tenerife, Spain*

³*Consejo Superior de Investigaciones Científicas, 28006 Madrid, Spain*

(Received December 19, 2017)

ABSTRACT

We report the discovery of the carbon-rich ultra metal-poor unevolved star J0815+4729. This dwarf star was selected from SDSS/BOSS as a metal-poor candidate and follow-up spectroscopic observations at medium-resolution were obtained with ISIS at William Herschel Telescope and OSIRIS at Gran Telescopio de Canarias. We use the FERRE code to derive the main stellar parameters, $T_{\text{eff}} = 6215 \pm 82$ K, and $\log g = 4.7 \pm 0.5$, an upper limit to the metallicity of $[\text{Fe}/\text{H}] \leq -5.8$, and a carbon abundance of $[\text{C}/\text{Fe}] \geq +5.0$, while $[\alpha/\text{Fe}] = 0.4$ is assumed. The metallicity upper limit is based on the Ca II K line, that at the resolving power of the OSIRIS spectrograph cannot be resolved from possible interstellar calcium. The star could be the most iron-poor unevolved star known, and is also amongst the ones with the largest overabundances of carbon. High-resolution spectroscopy of J0815+4729 will certainly help to derive other important element abundances, possibly providing new fundamental constraints on the early stages of the Universe, the formation of the first stars and the properties of the first supernovae.

Keywords: stars: PopulationII – stars: abundances – stars: PopulationIII – Galaxy:abundances –
Galaxy:formation – Galaxy:halo

Corresponding author: David S. Aguado
aguado@iac.es

* Based on observations made with the Gran Telescopio Canarias (GTC), installed in the Spanish Observatorio del Roque de los Muchachos of the Instituto de Astrofísica de Canarias, on the island of La Palma. Program ID GTC90-15B and the Discretionary Director Time GTC03-16ADDT.

1. INTRODUCTION

The existence of surviving population III stars is still under debate. The issue is intimately linked to the minimum mass at which a star can form at zero metallicity. Second generation stars are formed from matter polluted by the first supernovae; their chemical composition reflects the yields from the first massive stars. We can study the early chemical evolution of the Universe through the analysis of those second-generation low-mass stars. Stellar archeology has a deep impact in several fields of modern astrophysics, from stellar formation and evolution, to near-field cosmology. To make progress, it is necessary to identify larger samples of primitive stars and derive their chemical abundances.

The number of known extremely metal-poor stars has dramatically increased since the 80's. G64-12 with $[\text{Fe}/\text{H}] = -3.2^1$ was discovery by [Carney & Peterson \(1981\)](#), but these authors originally reported a metallicity of $[\text{Fe}/\text{H}] = -3.52$. Nowadays, a few hundred stars are cataloged as having $[\text{Fe}/\text{H}] < -3.0$ (see e.g. [Beers & Christlieb \(2005\)](#); [Aoki et al. \(2006\)](#); [Caffau et al. \(2013\)](#); [Norris et al. \(2013\)](#); [Yong et al. \(2013\)](#); [Placco et al. \(2015\)](#); [Aguado et al. \(2016\)](#) and references therein).

The first ultra metal-poor star ($[\text{Fe}/\text{H}] < -4.0$) was spectroscopically studied by [Bessell & Norris \(1984\)](#): CD $-38^\circ 245$, with $[\text{Fe}/\text{H}] = -4.5$. Recent studies by [Yong et al. \(2013\)](#) derive a metallicity of $[\text{Fe}/\text{H}] = -4.15$ for this star. Nearly thirty ultra metal-poor stars are already known (see e.g. [Bonifacio et al. \(2012\)](#); [Roederer et al. \(2014\)](#); [Yong et al. \(2013\)](#); [Hansen et al. \(2014\)](#); [Bonifacio et al. \(2015\)](#); [Placco et al. \(2015\)](#); [Allende Prieto et al. \(2015\)](#); [Aguado et al. \(2017b\)](#) and references therein). [Christlieb et al. \(2002, 2004\)](#) reported from Hamburg/ESO survey the discovery of HE 0107-5240 with a derived metallicity of $[\text{Fe}/\text{H}] = -5.39$ (LTE value). Since then, four more metal-poor stars below $[\text{Fe}/\text{H}] = -5$ have been detected: HE 1327-2326 with $[\text{Fe}/\text{H}] = -5.65$ ([Frebel et al. 2005](#); [Aoki et al. 2006](#)); J1035+0641 with $[\text{Fe}/\text{H}] < -5.07$ ([Bonifacio et al. 2015](#)) from the Sloan Sky Digital Survey (SDSS) ([York et al. 2000](#)); SMSS J01313-6708 with no iron features detected and $[\text{Fe}/\text{H}] < -7.20$ ([Keller et al. 2014](#)), and finally J1029+1729 ([Caffau et al. 2011](#)) with $[\text{Fe}/\text{H}] = -5.0$ but no measurable carbon abundance ($[\text{C}/\text{Fe}] < +0.7$).

With the exception of J1029+1729, all known metal-poor stars at $[\text{Fe}/\text{H}] < -4.5$, including J0815+4729, are carbon-enhanced metal-poor stars (CEMP). The

¹ We use the bracket notation for reporting chemical abundances: $[a/b] = \log\left(\frac{N(a)}{N(b)}\right) - \log\left(\frac{N(a)}{N(b)}\right)_\odot$, where $N(x)$ represents number density of nuclei of the element x .

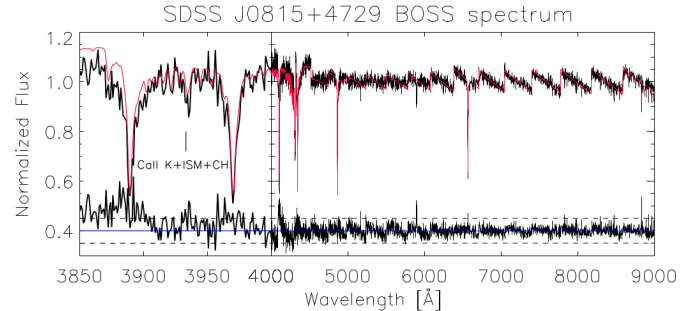


Figure 1. BOSS spectrum of J0815+4729 (black line) and the best fit obtained with FERRE (red line), after dividing the spectra in segments of about $\sim 300\text{-}400\text{\AA}$ which are normalized by their average fluxes. The residuals are shown in the lower panel.

observed increase in the frequency of CEMP stars at the lowest metallicities (see, e.g. [Cohen et al. 2005](#); [Placco et al. 2014](#)) could be explained by the fall-back mechanism in core-collapse supernovae (SN) ([Umeda & Nomoto 2003](#)) which is an easy way to get high C and low Fe out into the interstellar medium in the early universe. This effect is most relevant for zero-metallicity supernova progenitors (e.g. [Limongi et al. 2003](#)). In addition, [Cooke & Madau \(2014\)](#) suggest the importance of the ability of the host minihalos to retain their gas reservoir in order to explain the chemical composition observed in second-generation stars.

The calcium K resonance line is the strongest detectable metallic absorption line in the visible spectrum (see e.g. [Beers et al. 1992](#)). This line allows us to derive a metallicity estimate assuming $[\alpha/\text{Fe}] = 0.4$, even when iron lines are not detected, using medium resolution spectroscopy ([Aguado et al. 2017b,a](#)). In this work we report the discovery of J0815+4729, a new carbon-rich ultra metal-poor dwarf star with $[\text{Fe}/\text{H}] \leq -5.8$. The target identification and observations are explained in Section 2. The determination of atmospheric parameters is described in Section 3 together with a complete analysis of two comparison well-known metal-poor stars, G64-12 and J1313-0019. The discussion and the conclusions are given in Section 4.

2. TARGET SELECTION AND OBSERVATIONS

We analyzed more than 2.5 million low-resolution spectra from the Sloan Extension for Galactic Understanding and Exploration (SEGUE, [Yanny et al. 2009](#)), the Baryonic Oscillations Spectroscopic Survey (BOSS, [Eisenstein et al. 2011](#); [Dawson et al. 2013](#)) and the large Sky Area Multi-Object Fiber Spectroscopic Telescope (LAMOST, [Deng et al. 2012](#)). We derived a first set of stellar parameters: effective temperature, surface grav-

ity, metallicity and carbon abundance (see Section 3). This methodology allowed us to build a catalogue of ~ 100 metal-poor candidates to observe using medium-resolution follow-up spectroscopy with the Intermediate dispersion Spectrograph and Imaging System (ISIS) at the 4.2m William Herschel Telescope (WHT) (Aguado et al. 2016, 2017b) in the *Observatorio del Roque de los Muchachos* (La Palma, Spain). Our first analysis of the BOSS spectrum of J0815+4729 (R.A.= 08^h15^m54^s.25, DEC.=+47^o29′47″.85 (J2000), mag(g)=17.06±0.01 and $v_{rad} = -118 \pm 5 \text{ km s}^{-1}$.) with FERRE ² provided the parameters $T_{\text{eff}} = 6365 \text{ K}$, $\log g = 4.9$, $[\text{Fe}/\text{H}] = -4.6$ and $[\text{C}/\text{Fe}] = +3.9$, with FERRE internal uncertainties of 19 K; 0.06; 0.10 dex; 0.09 dex, respectively (see Figure 1). J0815+4729 was selected as a promising candidate to be extremely metal-poor as inferred in the FERRE analysis from the weak absorption shown in the region of the calcium K line. Further details about the selection candidates could be found in Aguado et al. (2017b).

Some obvious imperfections in the normalization of the BOSS spectrum probably caused by issues with the flux calibration together with significant noise in the vicinity of the calcium K line warranted a spectrum of higher S/N. The ISIS observations were obtained between Dec 31, 2014 - Jan 2, 2015, program C103. The set-up adopted the R600B and R600R gratings, the GG495 filter in the red arm and the default dichroic (5300 Å). The mean resolving power using a 1"slit was $R \sim 2400$ in the blue arm and $R \sim 5200$ in the red arm. Six individual exposures of 1800s were taken to avoid a significant degradation of the data due to cosmic rays and a coadded spectrum of S/N ~ 55 was obtained. In addition, two other well-studied metal-poor stars, G64-12 and J1313-0019 were observed for calibrating purposes (See Fig. 2) and details of the observations are provided in Aguado et al. (2017b).

After the analysis of the ISIS spectrum confirmed a very low metallicity we decided to obtain new spectrum with a much higher signal-to-noise ratio using the 10.4m Gran Telescopio Canarias (GTC) telescope equipped with the Optical System for Imaging and low-intermediate-Resolution Integrated Spectroscopy (OSIRIS) instrument. This allowed us to secure a S/N>200 spectrum in a reasonable amount of time.

The observations were scheduled in service mode during the Feb 13, 2016 night as part of the GTC90-15B program and Mar 27, 2016 in GTC03-16ADDT program. The sky requirements were in both cases a seeing with a FWHM< 1.2" and gray conditions. We se-

lected the R2500U grism of OSIRIS and a 1"slit, providing a spectral range 3600-4500 Å with a resolving power $R \sim 2500$. Ten exposures of 1584s were taken with identical set-up and similar sky conditions. For both the ISIS and the OSIRIS data reduction (bias subtraction, flat-fielding and wavelength calibration, using CuNe + CuAr lamps) we adopted the *onespec* package in IRAF³ (Tody 1993). For further details see Aguado et al. (2016, 2017b).

3. ANALYSIS

The analysis of J0815+4729 was carried out as explained in Aguado et al. (2017b,a). We used the grid of synthetic spectra (Aguado et al. 2017b) already available from CDS⁴. The grid was computed with the ASS ϵ T code (Koesterke et al. 2008) and uses the Barklem theory for self-broadening of the Balmer lines and the stark-broadened profiles from Stehle & Fouquet (2010). Model atmospheres were computed with ATLAS9 (Kurucz 1979) as described by Mészáros et al. (2012).

We assumed $[\alpha/\text{Fe}] = 0.4$ as a canonical value for the Galactic halo (Yong et al. 2013). The most metal-poor stars known ($[\text{Fe}/\text{H}] \lesssim -4.5$) typically show 1D-LTE abundance ratios $[\text{CaII}/\text{Fe}] \sim 0.25 - 0.4$ dex Christlieb et al. (2004); Hansen et al. (2014); Allende Prieto et al. (2015); Frebel et al. (2015); Bonifacio et al. (2015). Caffau et al. (2012) estimate $[\text{Ca II}/\text{Fe}] \sim 0.13$, while Frebel et al. (2008) get $[\text{Ca II}/\text{Fe}] \sim 0.7$, for their stars. On the other hand, Fernández-Alvar et al. (2015) found that $[\text{Ca}/\text{Fe}]$ depends on $[\text{Fe}/\text{H}]$ and distance r to the Galactic center, with higher values at lower $[\text{Fe}/\text{H}]$ and slightly increasing at distances $r > 20$ kpc, in the range 0.4-0.6 dex. Following Fernández-Alvar et al. (2015, and references therein), we estimate a distance to the star of ~ 2.3 kpc and a Galactocentric distance of ~ 10 kpc. Therefore, it seems reasonable to assume for J0815+4729 that $[\text{Ca}/\text{Fe}] \sim 0.4$. Synthetic spectra for metallicities below $[\text{Fe}/\text{H}] = -5$ were computed using model atmospheres with $[\text{Fe}/\text{H}] = -5$. The limits of the grid of synthetic spectra adopted in our analysis are $4750 \text{ K} \leq T_{\text{eff}} \leq 7000 \text{ K}$, $-6 \leq [\text{Fe}/\text{H}] \leq -2$; $+1 \leq [\text{C}/\text{Fe}] \leq +5$, and $1.0 \leq \log g \leq 5.0$ and a microturbulence ξ of 2 km s^{-1} was adopted. The FERRE code is able to derive simultaneously the stellar param-

³ IRAF is distributed by the National Optical Astronomy Observatory, which is operated by the Association of Universities for Research in Astronomy (AURA) under cooperative agreement with the National Science Foundation

⁴ The model spectra are only available at the Centre de Données astronomiques de Strasbourg (CDS) via anonymous ftp to cdsarc.u-strasbg.fr (130.79.128.5) or via http://cdsarc.u-strasbg.fr/viz-bin/qcat?J/A+A/605/A40

² FERRE is available from <http://github.com/callendeprieto/ferre>

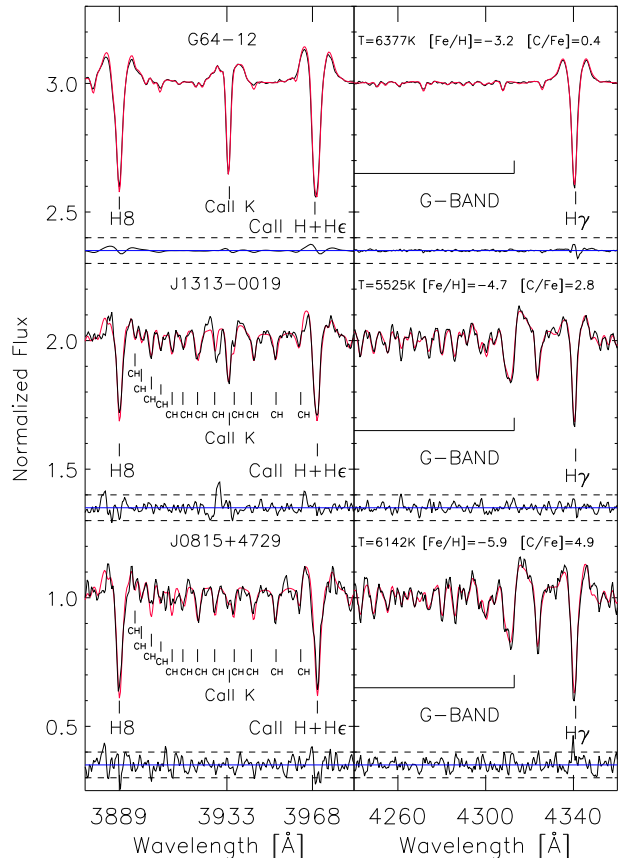


Figure 2. ISIS/WHT spectra of the G-band and Ca II lines of the stars J0815+4729, J1313-0019 and G64-12 (black line) and the best fit calculated with FERRE (red line). Both the observed and synthetic spectra have been normalized with a running-mean filter with a width of 30 pixels. The normalized spectra are vertically shifted for clarity. The residuals (difference between the observed spectrum and the best fit) are displayed under each spectrum, and the dashed lines correspond to differences of +5% and -5%. The effective temperature, metallicity and carbon abundance for each spectrum are also displayed.

eters, including metallicity, and the carbon abundance. The observed and synthetic spectra are normalized with a running-mean filter with a width 30 pixels (see Aguado et al. (2017b) for further details).

3.1. ISIS Analysis

The ISIS spectrum shows a myriad of CH transitions. These must be properly modeled to perform a thorough study of the Ca II K line at 3933 Å which is also blended with a interstellar medium (ISM) contribution. Most halo stars with metallicities $[\text{Fe}/\text{H}] < -4.5$ show interstellar calcium absorption. That fact could be partially explained due most of they are at large distances. A Gaussian profile was adopted to model the calcium ISM

contribution constructing a grid of absorption features running from 5% to 30% with a step of 1%, and relative velocities (Δv) from +70 km s⁻¹ to +110 km s⁻¹ with a step of 5 km s⁻¹, until we got the best χ^2 , and the resulting spectrum was reanalyzed with FERRE. The minimum χ^2 corresponds to a 28% the ISM contribution to the stellar Ca II K line at $\Delta v = +100$ km/s.

Figure 2 shows the ISIS spectrum of J0815+4729 together with other two well-known metal-poor stars, J1313-0019 and G64-12, also analyzed in Aguado et al. (2017b). The right-hand side of the panel shows the G-band area. The stars J1313-0019 and J0815+4729 show a strong G-band whereas G64-12, according with Aguado et al. (2017b), is not carbon-enhanced. The CH features in J0815+4729 are indeed stronger than in J1313-0019 despite the latter is almost 600 K cooler. The left-hand panels show the Ca II K line for these three stars. From the ISIS analysis we arrive at $T_{\text{eff}} = 6142 \pm 118$ K; $\log g = 4.7 \pm 0.6$; $[\text{C}/\text{Fe}] = 4.9 \pm 0.2$ dex; and with the Ca II K ISM feature at $\Delta v = +100$ km/s, $[\text{Fe}/\text{H}] = -5.9 \pm 0.2$ dex for J0815+4729. The derived radial velocity of the star is $v_{\text{rad}} = -83 \pm 38$ km s⁻¹.

3.2. OSIRIS analysis

The much higher S/N of the OSIRIS spectrum allows us to better model the ISM contribution. The methodology followed is the same explained in 3.1 and led to a more reliable value of 25% absorption at $\Delta v = +95$ km/s, corresponding to an equivalent width of ~ 30 mÅ. Figure 3 shows the entire OSIRIS spectrum of J0815+4729 (upper-left panel) and the best fit derived with FERRE. Without subtracting the ISM contribution (See Fig. 3, upper-right panel) FERRE is not able to model the blended line, thus overestimating the metallicity to be $[\text{Fe}/\text{H}] = -5.0$. The Ca II H&K and G-band spectral regions are displayed in the bottom panel. The radial velocity obtained from the OSIRIS spectrum by a cross correlation is $v_{\text{rad}} = -95 \pm 23$ km s⁻¹. The radial velocity values from the three spectra suggest no variation. The goodness of fit for the OSIRIS spectrum is remarkably good with a $\chi^2 = 1.1$, leading to the values $T_{\text{eff}} = 6215 \pm 82$ K, $\log g = 4.7 \pm 0.5$, $[\text{Fe}/\text{H}] \leq -5.8$ dex and a carbon abundance of $[\text{C}/\text{Fe}] \geq +5.0$. At this extremely low metallicity, the majority of the information on metallicity is coming from the Ca II K line, which provides an upper limit of $[\text{Ca}/\text{H}] < -5.4$ for J0815+4729. Since the structure of the ISM contribution could be more complicated than a separated single Gaussian component, and there could be more ISM components closely blended with the Ca II K stellar feature (see e.g. Frebel et al. 2005; Caffau et al. 2011; Aguado et al.

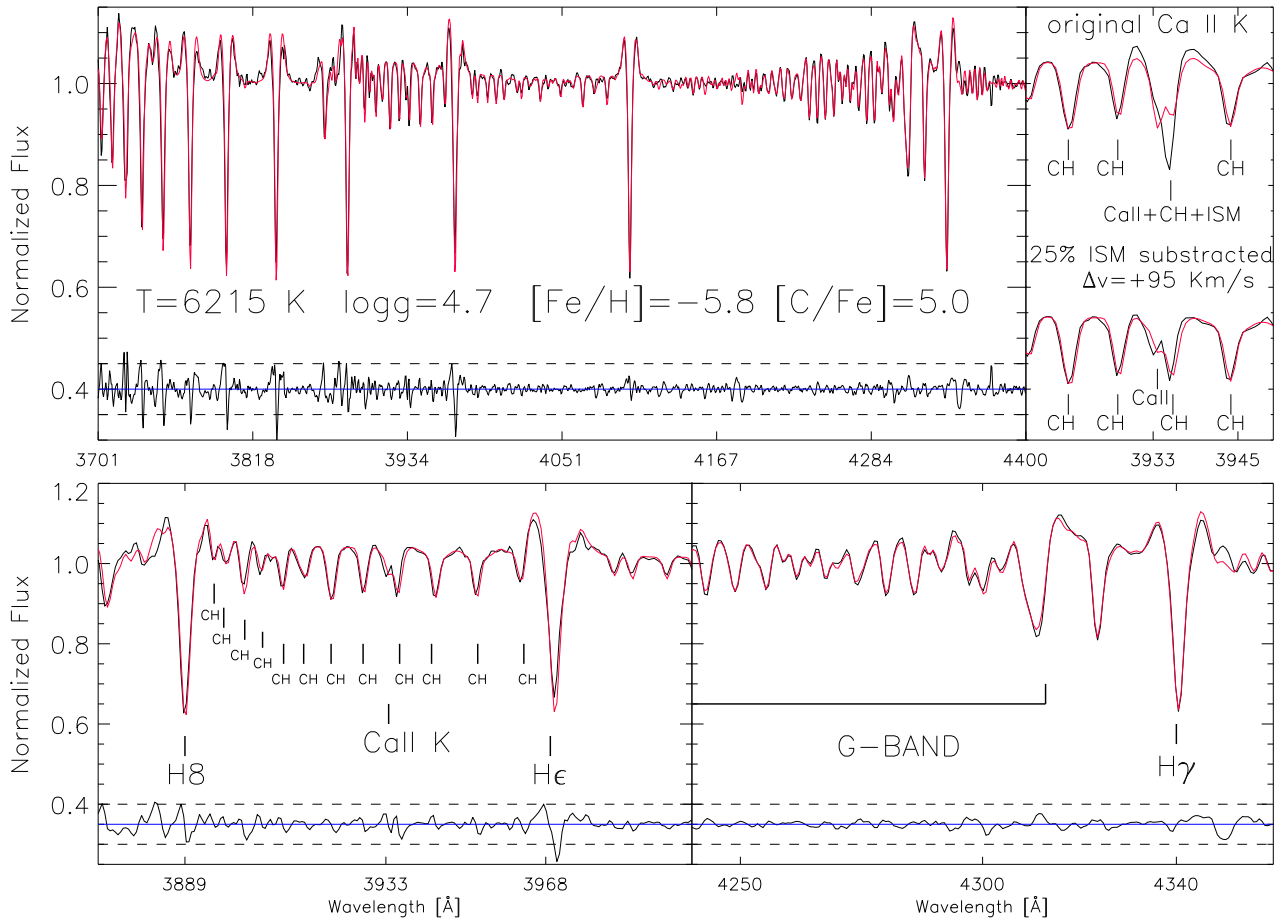


Figure 3. OSIRIS medium-resolution spectrum of J0815+4729 (black line) and the best fit obtained with FERRE (red line). The residuals (difference between the observed spectrum and the best fit) are shown underneath each of the spectra, together with the $\pm 5\%$ reference lines. The upper-right panel shows the original spectrum in the vicinity of the Ca II K line (top spectrum), and the same area after subtracting the ISM contribution (bottom).

2017b), we consider the calcium abundance and, consequently, the metallicity value derived from the Ca II K line as an upper limit.

Small traces of Fe I lines can be observed in the blue part of the OSIRIS spectrum (3815–3860 Å). Unfortunately, these features are too weak to derive an iron abundance at the OSIRIS resolution. However, we compare in Figure 4 (upper panel) models with different iron abundances and the original spectrum. It is clear that J0815+4729 is an iron-poor star with, at least, $[\text{Fe}/\text{H}] < -4.5$. J0815+4729 is the second most carbon-rich metal-poor star after SMSS J0313–6708 (Keller et al. 2014), which shows $[\text{C}/\text{Fe}] > 5.4$ with a metallicity of $[\text{Fe}/\text{H}] < -7.2$ derived from the non-detection of the strongest Fe lines and $[\text{Ca}/\text{H}] = -7.2$ derived from the

Ca II K line. Our analysis has been performed assuming a microturbulence $\xi = 2.0 \text{ km s}^{-1}$ instead of the more suitable value for dwarf stars of $\xi \sim 1.5 \text{ km s}^{-1}$ (see e.g. Cohen et al. 2004; Barklem et al. 2005). We have done a simple test to evaluate the impact of this assumption. We analyzed with FERRE both synthetic spectra computed with the same stellar parameters of J0815+4729 but with two different ξ values, 2.0 and 1.0 km s^{-1} . The variation in metallicity is small (0.06 dex) and the direction of higher metallicity with $\xi = 1.0 \text{ km s}^{-1}$, as expected. This result is consistent with the derived upper limit $[\text{Fe}/\text{H}] \leq -5.8$.

4. DISCUSSION AND CONCLUSIONS

J0815+4729 is a main-sequence star ($T_{\text{eff}} = 6215 \pm 82 \text{ K}$, $\log g = 4.7 \pm 0.5$) with a metallicity of $[\text{Fe}/\text{H}] \leq$

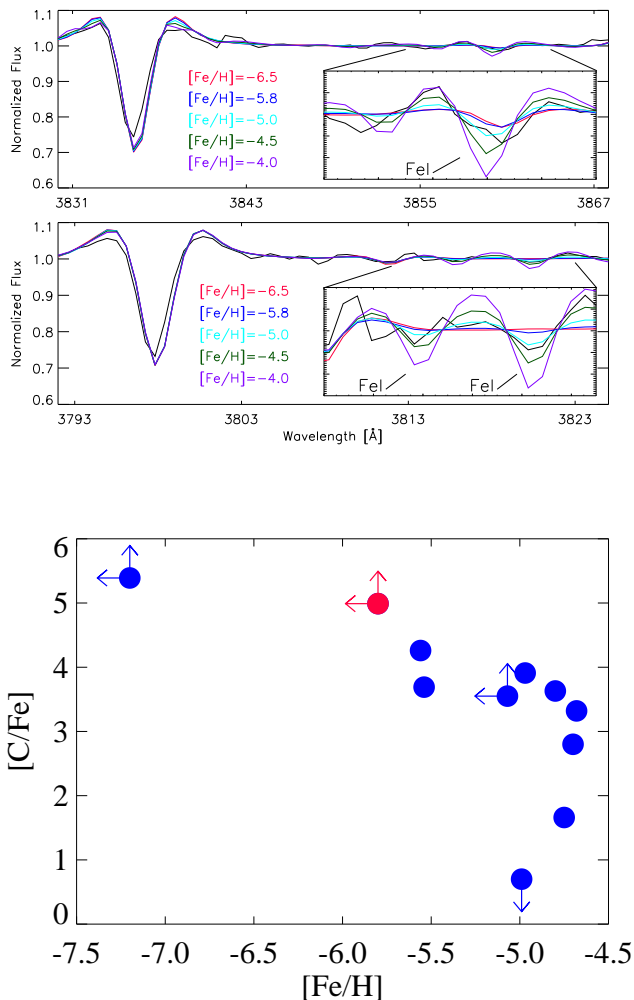


Figure 4. Upper panel: A detail of the OSIRIS J0815+4729 spectrum (black line) in the region covering strongest Fe I transitions (3815, 3820 and 3859 Å). Five synthetic spectra with different metallicities are also shown. Bottom panel: Carbon-to-iron ratio vs. iron abundance in the ten stars in the $[\text{Fe}/\text{H}] < -4.5$ regime already in the literature: Christlieb et al. (2004); Frebel et al. (2005); Norris et al. (2007); Caffau et al. (2011); Hansen et al. (2014); Keller et al. (2014); Allende Prieto et al. (2015); Bonifacio et al. (2015). J0815+4729 is marked in red.

−5.8 dex. Finding unevolved stars at this extremely low metallicity is very important since their stellar surface composition is not expected to be significantly modified by any internal mixing processes as in giant stars (Spite et al. 2005). J0815+4729 is similar to HE 1327–2326 in regards to its carbon enhancement, effective temperature and metallicity. HE 1327–2326 is considered a turn-off/subgiant star, while J0815+4729 appears to be

a dwarf. The ISIS spectrum of HE 1327–2326 indicates a metallicity of $[\text{Fe}/\text{H}] \sim -4.9$, since stellar Ca line is blended in that spectrum with the ISM features (Aguado et al. 2017b). However the authors proposed a simple analysis of the ISM effect based on the UVES spectrum of HE 1327–2326. For J0815+4729, we require a high-resolution spectrum to clearly isolate the stellar Ca feature from possible additional ISM lines, and thus, together with the detection of Fe lines, to establish the metallicity of this star. There are two other confirmed dwarf stars in this metallicity regime: one without any detectable carbon, J1029+1729 (Caffau et al. 2011), and another carbon enhanced unevolved star, J1035+0641 (Bonifacio et al. 2015). The majority of extremely metal-poor stars show overabundances of carbon, $[\text{C}/\text{Fe}] > 0.7$, and it appears that carbon enhanced metal-poor (CEMP) stars split into two groups, with dramatically different carbon abundances (see e.g. Beers & Christlieb (2005); Bonifacio et al. (2015); Allende Prieto et al. (2015) and references therein). The two carbon-bands (high and low) studied have different origins. On the one hand, CEMP stars in the high-carbon band ($A(\text{C}) \sim 8.2$) are probably produced by mass transfer from a binary companion, most likely an AGB star (Starkenburg et al. 2014). On the other hand, objects lying in the low-carbon-band ($A(\text{C}) \sim 6.8$) are thought to show the original carbon abundance inherited by the star from the interstellar medium (Stancliffe 2009; Abate et al. 2016; Bonifacio et al. 2015). J0815+4729 has an abundance ratio of $[\text{C}/\text{Fe}] \geq +5.0$ dex corresponding to $A(\text{C}) \sim 7.7$ dex (adopting $[\text{Fe}/\text{H}] \leq -5.8$). In Figure 4 (bottom panel) we show the carbon abundance ratio $[\text{C}/\text{Fe}]$ for all stars below $[\text{Fe}/\text{H}] < -4.5$. All stars in this metallicity regime are considered to belong to the low-carbon band (Bonifacio et al. 2015), except for J0815+4729, which appears to be in between the low- and high-carbon bands. Both metallicity and carbon abundance are considered upper and lower limits, respectively. High-resolution spectra would be very useful to measure other elemental abundances and investigate the properties of the first supernovae. In particular the barium abundance, or that of any other s-element is not measurable from ISIS or OSIRIS spectra, and this is required to determine whether J0815+4729 is a CEMP-s, CEMP-r or i-process star (Hampel et al. 2016). If we establish the abundance pattern we will learn about the progenitor properties. Finally, the radial velocity accuracy from medium-resolution data is not enough to discard variations among different exposures, which would be indicative of binarity.

The discovery of J0815+4729 starts to fill in the gap in iron abundance between SMSS J01313–6708 and the

rest of the extremely metal-poor stars. Identifying and characterizing chemically these rare breed of stars will certainly shed light on the early chemical evolution of the Galaxy and the nature of the first stars.

DA acknowledges the Spanish Ministry of Economy and Competitiveness (MINECO) for the financial support received in the form of a Severo-Ochoa PhD fellowship, within the Severo-Ochoa International PhD Program. DA, CAP, JIGH, and RR also acknowledge the Spanish ministry project MINECO AYA2014-56359-P. JIGH acknowledges financial support from the Spanish Ministry of Economy and Competitiveness (MINECO) under the 2013 Ramón y Cajal program MINECO RYC-2013-14875. The authors thankfully

acknowledge the technical expertise and assistance provided by the Spanish Supercomputing Network (Red Espanola de Supercomputación) and Antonio Dorta in particular, as well as the computer resources used: the LaPalma Supercomputer, located at the Instituto de Astrofísica de Canarias. This paper is based on observations made with the Gran Telescopio de Canarias (GTC) and with the William Herschel Telescope, operated by the Isaac Newton Group at the Observatorio del Roque de los Muchachos, La Palma, Spain, of the Instituto de Astrofísica de Canarias. We would like to thank GRANTECAN and ING staff members for their efficiency during the observing runs. In particular, we thank to A. Cabrera Lavers and D. Reverte Payá for their help during OSIRIS observations.

REFERENCES

- Abate, C., Stancliffe, R. J., & Liu, Z.-W. 2016, *A&A*, 587, A50
- Aguado, D. S., Allende Prieto, C., González Hernández, J. I., et al. 2016, *A&A*, 593, A10
- Aguado, D. S., Allende Prieto, C., González Hernández, J. I., Rebolo, R., & Caffau, E. 2017a, *A&A*, 604, A9
- Aguado, D. S., González Hernández, J. I., Allende Prieto, C., & Rebolo, R. 2017b, *A&A*, 605, A40
- Allende Prieto, C., Fernández-Alvar, E., Aguado, D. S., et al. 2015, *A&A*, 579, A98
- Aoki, W., Frebel, A., Christlieb, N., et al. 2006, *ApJ*, 639, 897
- Barklem, P. S., Christlieb, N., Beers, T. C., et al. 2005, *A&A*, 439, 129
- Beers, T. C., & Christlieb, N. 2005, *Highlights of Astronomy*, 13, 579
- Beers, T. C., Preston, G. W., & Shectman, S. A. 1992, *AJ*, 103, 1987
- Bessell, M. S., & Norris, J. 1984, *ApJ*, 285, 622
- Bonifacio, P., Sbordone, L., Caffau, E., et al. 2012, *A&A*, 542, A87
- Bonifacio, P., Caffau, E., Spite, M., et al. 2015, *A&A*, 579, A28
- Caffau, E., Bonifacio, P., François, P., et al. 2011, *Nature*, 477, 67
- . 2012, *A&A*, 542, A51
- Caffau, E., Bonifacio, P., Sbordone, L., et al. 2013, *A&A*, 560, A71
- Carney, B. W., & Peterson, R. C. 1981, *ApJ*, 245, 238
- Christlieb, N., Gustafsson, B., Korn, A. J., et al. 2004, *ApJ*, 603, 708
- Christlieb, N., Wisotzki, L., & Graßhoff, G. 2002, *A&A*, 391, 397
- Cohen, J. G., Christlieb, N., McWilliam, A., et al. 2004, *ApJ*, 612, 1107
- Cohen, J. G., Shectman, S., Thompson, I., et al. 2005, *ApJL*, 633, L109
- Cooke, R. J., & Madau, P. 2014, *ApJ*, 791, 116
- Dawson, K. S., Schlegel, D. J., Ahn, C. P., et al. 2013, *AJ*, 145, 10
- Deng, L.-C., Newberg, H. J., Liu, C., et al. 2012, *Research in Astronomy and Astrophysics*, 12, 735
- Eisenstein, D. J., Weinberg, D. H., Agol, E., et al. 2011, *AJ*, 142, 72
- Fernández-Alvar, E., Allende Prieto, C., Schlesinger, K. J., et al. 2015, *A&A*, 577, A81
- Frebel, A., Chiti, A., Ji, A. P., Jacobson, H. R., & Placco, V. M. 2015, *ApJL*, 810, L27
- Frebel, A., Collet, R., Eriksson, K., Christlieb, N., & Aoki, W. 2008, *ApJ*, 684, 588
- Frebel, A., Aoki, W., Christlieb, N., et al. 2005, *Nature*, 434, 871
- Hampel, M., Stancliffe, R. J., Lugaro, M., & Meyer, B. S. 2016, *ApJ*, 831, 171
- Hansen, T., Hansen, C. J., Christlieb, N., et al. 2014, *ApJ*, 787, 162
- Keller, S. C., Bessell, M. S., Frebel, A., et al. 2014, *Nature*, 506, 463
- Koesterke, L., Allende Prieto, C., & Lambert, D. L. 2008, *ApJ*, 680, 764
- Kurucz, R. L. 1979, *ApJS*, 40, 1
- Limongi, M., Chieffi, A., & Bonifacio, P. 2003, *ApJL*, 594, L123

- Mészáros, S., Allende Prieto, C., Edvardsson, B., et al. 2012, *AJ*, 144, 120
- Norris, J. E., Christlieb, N., Korn, A. J., et al. 2007, *ApJ*, 670, 774
- Norris, J. E., Bessell, M. S., Yong, D., et al. 2013, *ApJ*, 762, 25
- Placco, V. M., Frebel, A., Beers, T. C., et al. 2014, *ApJ*, 781, 40
- Placco, V. M., Frebel, A., Lee, Y. S., et al. 2015, *ApJ*, 809, 136
- Roederer, I. U., Preston, G. W., Thompson, I. B., et al. 2014, *AJ*, 147, 136
- Spite, M., Cayrel, R., Plez, B., et al. 2005, *A&A*, 430, 655
- Stancliffe, R. J. 2009, *MNRAS*, 394, 1051
- Starkenburger, E., Shetrone, M. D., McConnachie, A. W., & Venn, K. A. 2014, *MNRAS*, 441, 1217
- Stehle, C., & Fouquet, S. 2010, *International Journal of Spectroscopy Volume 2010* (2010), 6 pages, id #506346, 2010, doi:10.1155/2010/506346
- Tody, D. 1993, in *Astronomical Society of the Pacific Conference Series*, Vol. 52, *Astronomical Data Analysis Software and Systems II*, ed. R. J. Hanisch, R. J. V. Brissenden, & J. Barnes, 173
- Umeda, H., & Nomoto, K. 2003, *Nature*, 422, 871
- Yanny, B., Rockosi, C., Newberg, H. J., et al. 2009, *AJ*, 137, 4377
- Yong, D., Norris, J. E., Bessell, M. S., et al. 2013, *ApJ*, 762, 26
- York, D. G., Adelman, J., Anderson, Jr., J. E., et al. 2000, *AJ*, 120, 1579